



OPEN Variable fluid properties analysis for thermally laminated 3-dimensional magnetohydrodynamic non-Newtonian nanofluid over a stretching sheet

Noreen Sher Akbar^{1✉}, A. Al-Zubaidi², S. Saleem² & Shami A. M. Alsallami³

This article is mainly focused on the viscous flow of cu-water/Methanol suspended nanofluids towards a three-dimensional stretching sheet reformed by magnetohydrodynamic phenomenon. The viscous effect is considered as temperature dependent with water treated as a base fluid. Similarity conversions are employed to set forth the non-linear equations of this physical problem. An innovative model for 3D analysis for cu-water/Methanol nanofluid with an irregular viscosity is presented in the present study. Reynold's model of viscosity is considered in the present study. Moreover, shooting technique is employed to elaborate the non-linear coupled governing equations with the relevant boundary conditions. The physical interpretation of these numerical calculations is presented through a graphical specimen of velocity, Nusselt number, temperature, and skin friction etc. The results of present model are showing quality harmony with the results of existing model. This model is being used for manipulating and designing the surfaces such as stretching/shrinking wrapping and panting devices in nanotechnology. The results also show the significant changes in flow characteristics with changing the value of stretching parameter. It is observed that with an increasing in nanoparticles volume fraction boundary layer thickness decreases. Further, it is also observed that with an increase in viscosity parameter, temperature increases because here we are considering temperature dependent viscosity.

List of symbols

(u, v, w)	Velocity components, m/s, L/T
ax	Linear velocity in x direction, m/s, L/T
B_0	Magnitude of magnetic field, Tesla = Kg/s ² A, M/AT ²
u_w, v_w	Wall velocities, m/s, L/T
k_f	Thermal conductivity of the fluid, W/mK, ML/T ³ Θ ¹
T_w	Wall temperature, Kelvin, Θ
$\mu_{nf}(T)$	Temperature dependent viscosity of nanofluid, Ns/m ² , M/LT
ρ_f	Density of the base fluid, kg/m ³ , M/L ³
k_s	Thermal conductivity of the nanoparticles, W/mK, ML/T ³ Θ ¹
γ_f	Thermal expansion coefficient of base fluid, 1/K, I/T
γ_s	Thermal expansion coefficient of the nanoparticles, 1/K, I/T
γ_{nf}	Thermal expansion coefficient of nanofluid, 1/K, I/T
ρ_s	Density of the nanoparticles, kg/m ³ , M/L ³
k_f	Thermal conductivity of the base fluid, W/mK, ML/T ³ Θ ¹

¹DBS&H CEME, National University of Sciences and Technology, Islamabad, Pakistan. ²Department of Mathematics, College of Science, King Khalid University, Abha 61413, Saudi Arabia. ³Department of Mathematical Sciences, College of Applied Science, Umm Al-Qura University, Makkah 21955, Saudi Arabia. ✉email: noreen.sher@ceme.nust.edu.pk

(x, y, z)	Cartesian system of coordinates, m, L
b_y	Linear velocity in y direction, m/s, L/T
T_∞	Ambient temperature, Kelvin, Θ
$a, b > 0$	Balancing constants, 1/K, 1/T
T	Temperature, Kelvin, Θ
α_{nf}	Thermal diffusivity of nanofluid, $m^2/K, L^2/T$
α	Viscosity parameter (1)
λ	Ratio of stretching velocities in the y- and x-directions (1)
M	Hartmann number (1)
θ	Temperature in dimensionless form (1)
Pr	Prandtl number
φ	Nanoparticle volume fraction

There are many industrial requirements to manufacture the products which optimize the time, cost, space and pollution etc. to fulfill the worldwide needs. Works in the field of Nano science and nanotechnology has recently aided in the optimization of constraints in industrial and engineering requirements. Nowadays, there are many refinements and improvements in the field of nanoscience and technology which are reported by researchers and scientists. Nanofluid dynamics is a part of nanoscience where we study the effects of nanoparticles volume, energy distribution and accumulation with base fluid. The restoration of electronic equipment, vehicles temperature reduction, nuclear catalyst all includes the influence of nanotechnology. Generally, it reported that nanoparticles enhance the thermal conductivity of working fluids.

Das et al.¹ had illuminated the dramatic thermal enhancement effects of nanofluids with practical applications in material sciences, chemical engineering and physical sciences as well. Wang and Arun² had interpreted the impacts of nanofluids on the flow distribution and characteristics in both free and forced convection problems. Trisaksri and Wongwises³ had presented multiple techniques in their study to highlight the addition of nanoparticles and their impact on thermal enhancement. Murshed et al.⁴ had conducted a comparison of the experimental and analytical results of Nanofluid addition and thermal enhancement effects. Wang and Mujumdar⁵ had also narrated the theoretical aspects in addition to the numerical calculations for thermal enhancement and nanofluid addition. Kakac and Pramuanjaroenkij⁶ had conveyed a review study on the nanofluids heat distribution impacts on the forced convection problems. Wen et al.⁷ had provided practical applications on this fascinating topic of heat distribution enhancement with Nanofluids, as well as its limitations. Yu and Xie⁸ had explained the multiple methods of nanofluid preparation, the stability of nanofluids and some practical applications in their research review. Some other key research works that illustrate the impact of heat distribution enhancement via Nano fluids and their applications are^{9–13}. Akbar et al.^{14,15} had provided a mathematical model of the nanofluid effects on a vertically placed stretching surface under a magnetic field and uneven viscous impacts. They had also highlighted the applications of CNTs in biotechnology and micro-electronic appliances. Sheikholeslami and Chamkha¹⁶ had numerically investigated the electric field effects on the natural convection of nanofluids via finite element technique. Uddin et al.¹⁷ had utilized the Lie-group conversions for the first time for a bio-convection flow problem with nanofluidic impacts. Sheikholeslami and Chamkha¹⁸ had studied the uneven MHD effects on the lid driven cavity flow problem with enhanced nanofluid heat transfer effects. Kothandapani and Prakash¹⁹ had modeled the nanofluid effects on the peristaltic flow with radiation and porosity impacts. Brownian motion and thermophoresis are two key points of their research work. The magnetic field impact, hydro-thermal treatment via nanofluids, applications of nanofluids in micro-fluidic appliances and, cilia effects are narrated in following studies^{20–25}.

After a thorough review of the literature on nanofluids, it is observed that two-dimensional flow of nanofluids is reported in most of the studies, which do not cover the all industrial and nanotechnological applications. Some authors^{26–31} reported the three-dimensional flow analysis for nanofluids which are more relevant in application point of view in comparison to two-dimensional and one dimensional flows. Hayat et al.²⁶ had investigated the impact of nanofluid heat distribution on Visco-elastic models; Mahanthesh et al.²⁷ had reported 3D analysis for heat distribution impact of nanofluids with nonlinear radiations; Kolsi et al.²⁸ discussed the entropy generation nanofluids in three dimensional Buoyancy-Induced Flow; Khan et al.²⁹ presented numerical results for a heated deformable surface with nanofluids heat distribution; Khan et al.³⁰ extended their work for Burgers nanofluid. Zhu et al.³¹ numerically analyzed the convective heat distribution impacts enhanced via nanofluid addition inside a wavy conduit containing aluminum oxide and ethylene glycol nano particles. They have obtained the numerical solutions and found that the thermal conductivity of silver-water nanofluid enhances with increasing nanoparticle volume fraction and temperature but decreases for larger sized nanoparticles.

The investigation of boundary-layer theory for a stretching plane has intrigued many researchers and industry people because of its widespread applications in industry and nanotechnology. Such models are applicable in production of paper, plastic sheets firms, and fiber, glass production etc. Motivated by the huge range of industrial applications on stretching sheets flow problems with nanofluids, some authors^{32–34} have presented the 3D flow analysis of nanofluids considering different stretching geometries viz. bidirectional stretching surface, slandering stretching and stretching sheet. The MHD impacts in a 3D flow analysis for nanofluids through a nonlinear stretching surface and slandering stretching sheet was modeled by Nadeem et al.³⁵. Further literature can be view and analyzed through Refs.^{36–39}. Venkata et al.⁴⁰ had discussed the impact of Soret and Dufour on MHD Casson fluid flow past a stretching surface with convective diffusive conditions. They observed that depreciate temperature and appreciate concentration with the upsurge in Sorret number.

Numerous theoretical, experimental and numerical investigations on nanofluids have been reported in the last few years to progress the new technologies for the increasing heat distribution production of base fluids. There

are many sorts of nanoparticles that are distributed in base fluid and enhanced thermal conductivity is attained. Methanol is one of the most applicable nanoparticles that result in a very effective way to boost the thermal conductivity. Inspired from the combined effect of magnetic field and Methanol nanoparticles with Reynolds model of viscosity, a three-dimensional flow analysis for the stretching sheet is presented in this analysis. The motivation behind this work is that there is no previous work which reported combined analysis of nanoparticles with Reynolds mode of viscosity. As it is temperature dependent viscosity model. This model is being utilized in many industrial applications. Like sanitary fluid transport, blood pumps in heart lungs machine and transport of corrosive fluids etc. As for fluids in industry and in engineering prospectus fluids have variable fluid properties.

Formulation of the problem

An incompressible, laminar flow of CNTs is considered over a horizontally held sheet with stretching surface as shown in Fig. 1. A cartesian system (x, y, z) is used here with an even applied magnetic field side by side to z-axis.

After availing the boundary layer approximations, we have obtained the following set of equations for this flow problem:

$$\frac{\partial u}{\partial x} + \frac{\partial v}{\partial y} + \frac{\partial w}{\partial z} = 0, \tag{1}$$

$$\left(u \frac{\partial u}{\partial x} + v \frac{\partial u}{\partial y} + w \frac{\partial u}{\partial z} \right) = \frac{1}{\rho_{nf}} \frac{\partial}{\partial y} \left(\mu_{nf} * (T) \frac{\partial u}{\partial z} \right) - \frac{\sigma B_0^2}{\rho_{nf}} u, \tag{2}$$

$$\left(u \frac{\partial v}{\partial x} + v \frac{\partial v}{\partial y} + w \frac{\partial v}{\partial z} \right) = \frac{1}{\rho_{nf}} \frac{\partial}{\partial y} \left(\mu_{nf} * (T) \frac{\partial v}{\partial z} \right) - \frac{\sigma B_0^2}{\rho_{nf}} v, \tag{3}$$

$$\left(u \frac{\partial T}{\partial x} + v \frac{\partial T}{\partial y} + w \frac{\partial T}{\partial z} \right) = \alpha_{nf} \frac{\partial^2 T}{\partial z^2}, \tag{4}$$

The boundary conditions associated with the present problem are

$$u = u_w(x) = ax, v = v_w(y) = by, w = 0, T = T_w, \text{ at } z = 0, u \rightarrow 0, v \rightarrow 0, T \rightarrow T_\infty, \text{ as } z \rightarrow \infty \tag{5}$$

The properties of nanofluids with mathematical modeling are defined³⁷⁻³⁹ as:

$$\mu_{nf} = \frac{\mu_f e^{-\alpha\theta}}{(1 - \phi)^{2.5}}, \tag{6a}$$

$$\alpha_{nf} = \frac{k_{nf}}{(\rho c_p)_{nf}}, \rho_{nf} = (1 - \phi)\rho_f + \phi\rho_s, \tag{6b}$$

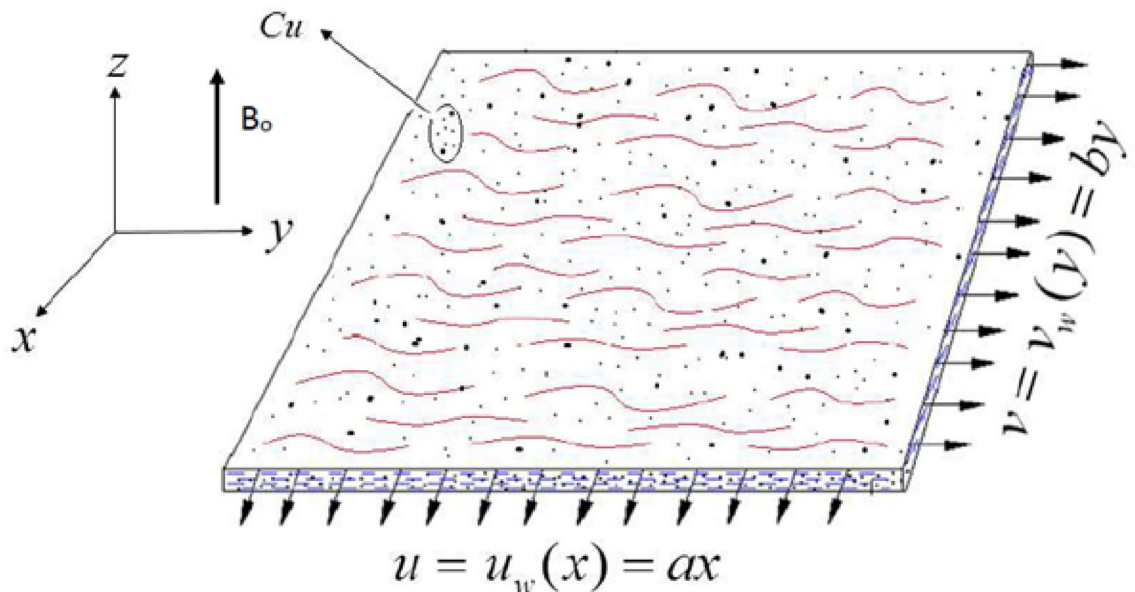


Figure 1. Geometry of the problem.

$$(\rho c_p)_{nf} = (1 - \varphi)(\rho c_p)_f + \varphi(\rho c_p)_s, \tag{6c}$$

$$(\rho \gamma)_{nf} = (1 - \varphi)(\rho \gamma)_f + \varphi(\rho \gamma)_s, \tag{6d}$$

$$k_{nf} = k_f \left(\frac{k_s + 2k_f - 2\varphi(k_f - k_s)}{k_s + 2k_f + 2\varphi(k_f - k_s)} \right) \tag{6e}$$

The similarity conversions availed in this analysis are given as:

$$\eta = \sqrt{\frac{a}{\nu_f}} z, u = axf'(\eta), v = byg'(\eta), \theta = \frac{T - T_\infty}{T_w - T_\infty}, w = \sqrt{\frac{\nu_f}{a}} (af(\eta) + bg(\eta)) \tag{7}$$

$$\mu_{nf} = \mu_{nf}^* \frac{\mu_o}{\mu_o}, M = B_0 \sqrt{\frac{a\sigma}{u_w \rho}}$$

Equations (1)–(5) convey the following reduced form after utilizing the Eqs. (6a–e, 7):

$$\frac{\mu_f(\theta)}{(1 - \varphi)^{2.5}} f'''' + \frac{1}{(1 - \varphi)^{2.5}} \mu_f'(\theta) f'' + \left[\left(1 - \varphi + \varphi \frac{\rho_s}{\rho_f} \right) \{ (f + \lambda g) f'' - f'^2 \} + M^2 f' \right] = 0, \tag{8}$$

$$\frac{\mu_f(\theta)}{(1 - \varphi)^{2.5}} g'''' + \frac{1}{(1 - \varphi)^{2.5}} \mu_f'(\theta) g'' + \left[\left(1 - \varphi + \varphi \frac{\rho_s}{\rho_f} \right) \{ (f + \lambda g) g'' - g'^2 \} + M^2 g' \right] = 0, \tag{9}$$

$$\left(\frac{k_{nf}}{k_f} \right) \theta'' + Pr \left(1 - \varphi + \varphi \frac{(\rho c_p)_s}{(\rho c_p)_f} \right) \left[(f\theta' + \lambda g) \right] = 0, \tag{10}$$

$$f(0) = 0, f'(0) = 1, f'(\infty) = 0, \tag{11a}$$

$$g(0) = 0, g'(0) = \lambda, g'(\infty) = 0 \tag{11b}$$

$$\theta(0) = 1, \theta(\infty) = 0, \tag{11c}$$

The dimensionless variables appeared here are provided as

$$Pr = \frac{(\mu_o c_p)_f}{k_f}, \lambda = b/a$$

The Reynold model used here for viscosity is³⁸:

$$\mu_f(\theta) = e^{-(\alpha\theta)} = 1 - (\alpha\theta) + O(\alpha^2), \tag{12}$$

Skin friction and Nusselt number.

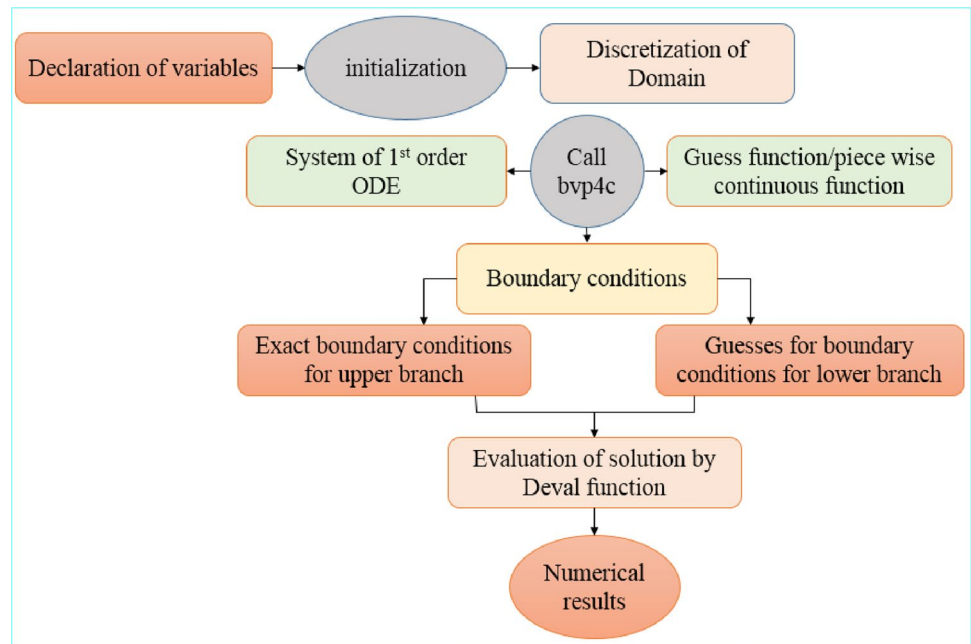
$$c_{fx} = \frac{\mu_{nf}(T)}{\rho_f u_w^2} \left(\frac{\partial u}{\partial z} \right)_{z=0}, c_{fy} = \frac{\mu_{nf}(T)}{\rho_f u_w^2} \left(\frac{\partial v}{\partial z} \right)_{z=0}, Nu_x = \frac{-xk_{nf}}{k_f(T_w - T_\infty)} \left(\frac{\partial T}{\partial z} \right)_{z=0} \tag{13}$$

Equation (13) in dimensionless form is given as

$$(Re_x)^{1/2} c_{fx} = \frac{\mu_f(\theta(0))f''(0)}{(1 - \varphi)^{2.5}}, (Re_y)^{1/2} c_{fy} = \lambda \left(\frac{y}{x} \right) \frac{\mu_f(\theta(0))g''(0)}{(1 - \varphi)^{2.5}}, (Re_x)^{1/2} Nu_x = -\frac{k_{nf}}{k_f} \theta'(0) \tag{14}$$

Numerical illustration

The shooting technique is employed to numerically expound Eqs. (8)–(10) with specific boundary conditions (11a–11c). The problem was fundamentally a boundary value (BVP) problem and to solve it via shooting technique, we have transformed it into an initial value (IVP) problem. The (RK) Runge Kutta technique with fourth order is employed with some initial guess values for $f''(0)$, $\theta'(0)$ and $g''(0)$ to acquire numerical solutions to the present problem. These initial guess values are better modified via Secant technique. The considered $\Delta\eta = 0.01$ is the step size here with a 5th decimal convergence.



Numerical code to evaluate the solutions is listed below.

```
restart;
```

```
odeSys :=  $\frac{1-(\alpha*\theta(y_i))}{(1-\varphi)^{2.5}} * \text{diff}(f(y_i), y_i, y_i, y_i) - \frac{\alpha}{(1-\varphi)^{2.5}} * \text{diff}(f(y_i), y_i, y_i) + (1 - \varphi + \varphi \frac{\rho_s}{\rho_f}) * (f(y_i) + \lambda * g(y_i)) \text{diff}(f(y_i), y_i, y_i) - \text{diff}(f(y_i), y_i)^2 + M^2 * \text{diff}(f(y_i), y_i) = 0,$ 
```

```
 $\frac{1-(\alpha*\theta(y_i))}{(1-\varphi)^{2.5}} * \text{diff}(g(y_i), y_i, y_i, y_i) - \frac{\alpha}{(1-\varphi)^{2.5}} * \text{diff}(g(y_i), y_i, y_i) + (1 - \varphi + \varphi \frac{\rho_s}{\rho_f}) * (f(y_i) + \lambda * g(y_i)) \text{diff}(g(y_i), y_i, y_i) - \text{diff}(g(y_i), y_i)^2 + M^2 * \text{diff}(g(y_i), y_i) = 0, \left(\frac{k_{nf}}{k_f}\right) \text{diff}(\theta(y_i), y_i, y_i) + Pr \left(1 - \varphi + \varphi \frac{(\rho c_p)_s}{(\rho c_p)_f}\right) [(f(y_i)\theta(y_i) + \lambda g(y_i))] = 0;$ 
```

```
bcs := f(0)=0, g(0)=0, fD(f)(infinity)=0, D(g)(infinity) =0, g(infinity)=0, theta(0) = 1, D(f)(0) = 1, D(g)(0) = lambda, theta(infinity) = 1;
```

```
inf:=100;
```

```
respar:=dsolve(eval({odeSys, f(0)=alpha, g(0)=0, D(f)(0)=f1}, {alpha=0.4, lambda =0.5, rho_s = 8933, rho_f = 997 }), numeric, parameters=[f1], output=listprocedure);
```

```
F:=subs(respar, f(y_i));
```

```
Q:=proc(f1) if not f1::realcons then return 'procname(_passed)' end if;
```

```
respar(parameters=[f1]);
```

```
F(inf)
```

```
end proc;
```

```
plot(f(y_i), y_i = 0..0);
```

Results and discussion

Figures 2, 3, 4, 5, 6 and 7 depict the graphical conclusions of temperature profile, skin friction, velocity, stream-lines and Nusselt number etc. The impact of M and α on the x -direction velocity profile is given by Fig. 2a and b with distinct $\phi = 0, 0.1, 0.2$ values. The highest velocity profile is observed at $\eta = 0$ while it diminishes as $\eta \rightarrow \infty$. A declining boundary layer thickness is noted for increasing nanoparticle volume. Further, the flow profile reduces or velocity declines with increasing numerical values of α . The viscosity in our case is varying with changing temperature distribution since a temperature dependent viscosity case is taken here. The incrementing α provides the risen viscous effects those results in enhanced temperature and reduced flow profile.

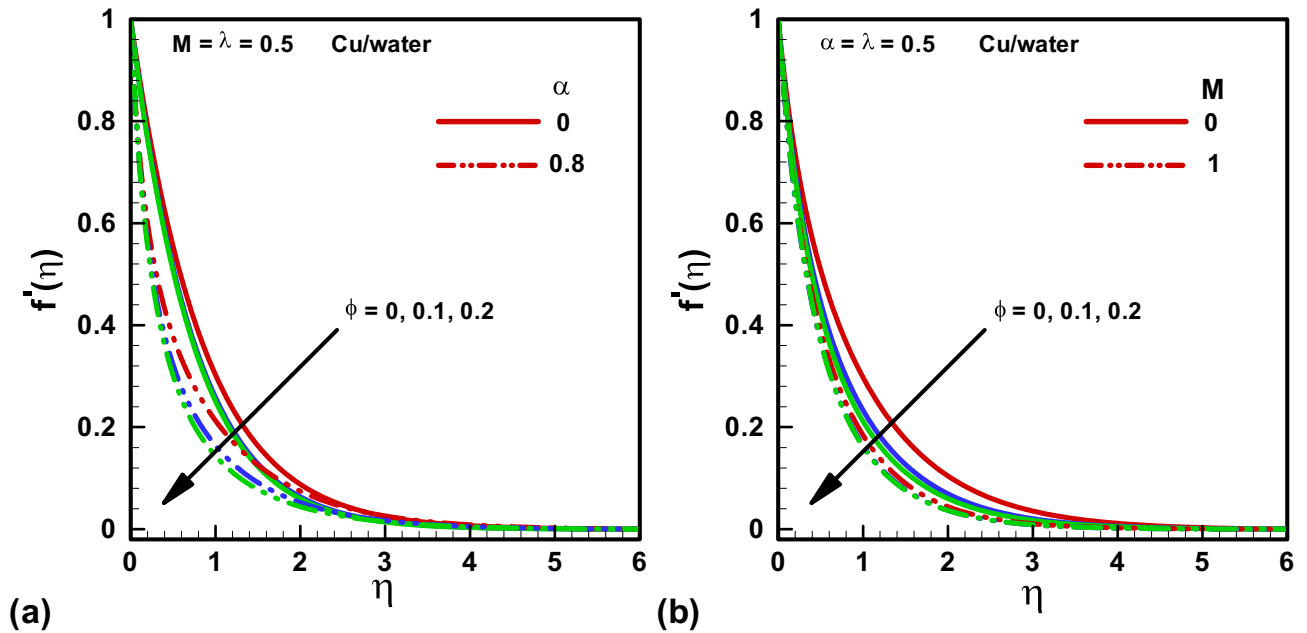


Figure 2. Velocity solutions x -direction for various ϕ . (a) $\alpha = 0, \alpha = 0.8$. (b) $M = 0, M = 1$. Red, Blue, Green Solid lines are for Methanol, Red, Blue, Green dotted lines are for water.

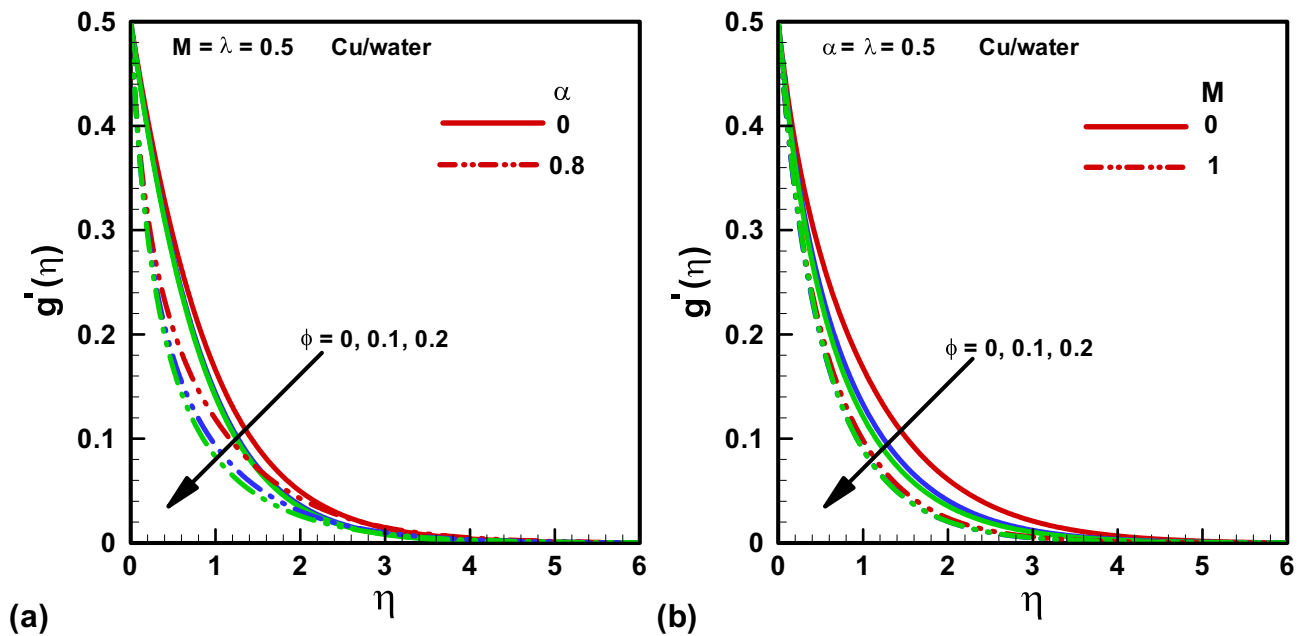


Figure 3. Velocity solutions in y -direction for various ϕ . (a) $\alpha = 0, \alpha = 0.8$. (b) $M = 0, M = 1$. Red, Blue, Green Solid lines are for Methanol, Red, Blue, Green dotted lines are for water.

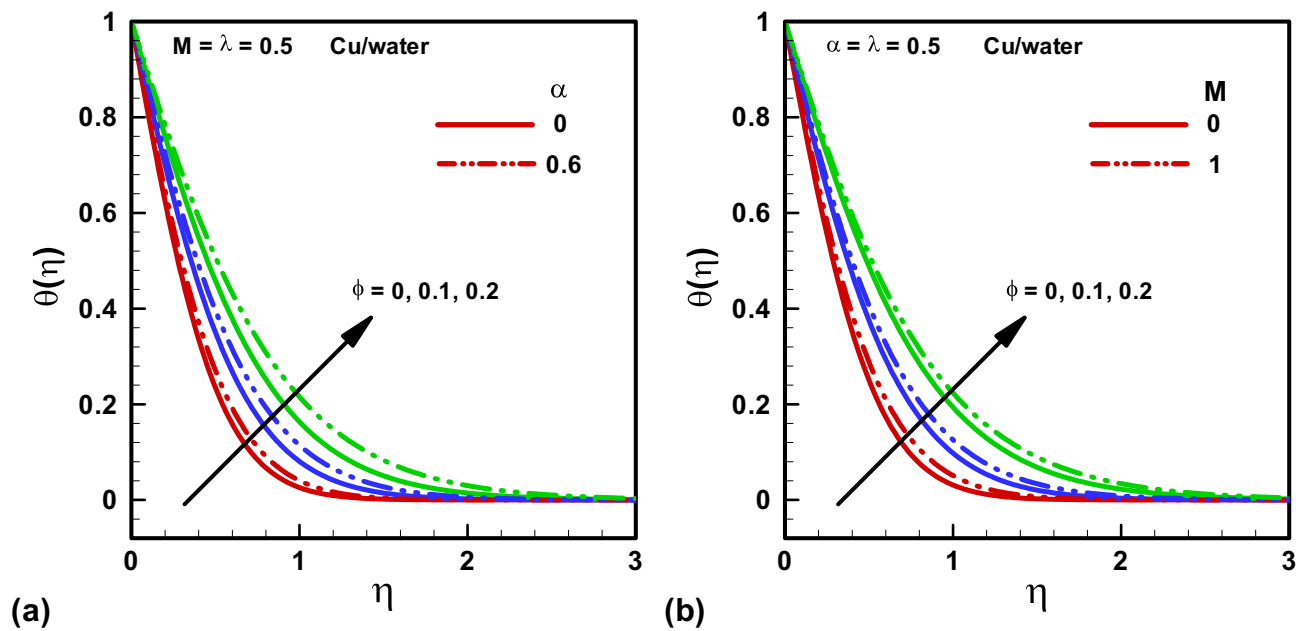


Figure 4. Temperature distribution for various ϕ with assisting and opposing flow considering. (a) $\alpha = 0$, $\alpha = 0.6$. (b) $M = 0$, $M = 1$. Red, Blue, Green Solid lines are for Methanol, Red, Blue, Green dotted lines are for water.

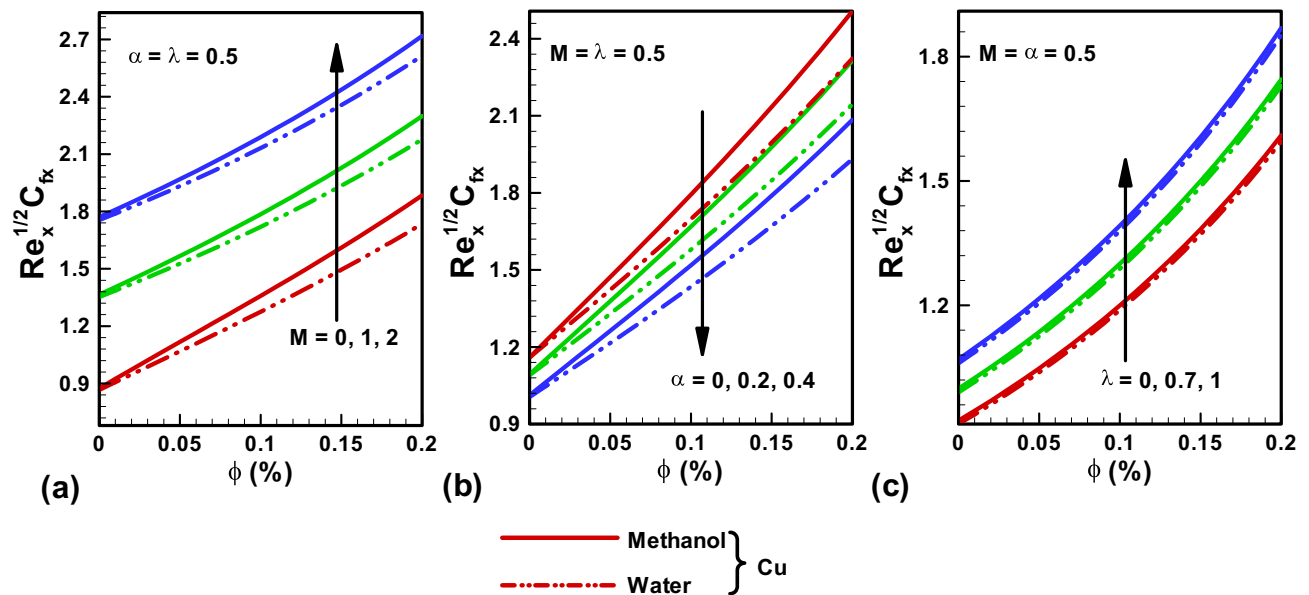


Figure 5. Skin friction results along x-direction (a) variable M . (b) variable α . (c) variable λ . Red, Blue, Green Solid lines are for Methanol, Red, Blue, Green dotted lines are for water.

Thus, a declining thickness of the boundary layer is noted. Figure 2b shows that the rising effects of Hartmann number M result in a declining flow profile because the Hartmann number M is the ratio of electromagnetic force to the viscous force. When we increase the Hartmann number electromagnetic force will be dominant to the viscous forces that will decline the velocity profile. Eventually the extent of boundary layer is reduced with incrementing M . Figure 3a and b convey the impact of Hartmann number M and viscosity parameter α on y -direction velocity profile with multiple values of $\phi = 0, 0.1, 0.2$. A similar behavior is noted for y -direction velocity profile as that of x -direction.

Figure 4a and b represent the graphical solutions of temperature profile for Hartmann number M and viscosity parameter α with distinct numerical values of ϕ . An increase in the temperature distribution is observed with distinct incrementing values of the viscosity parameter α . Because we are considered temperature dependent viscosity so increasing viscosity parameter α will definitely increase temperature profile. Further, an increase in the

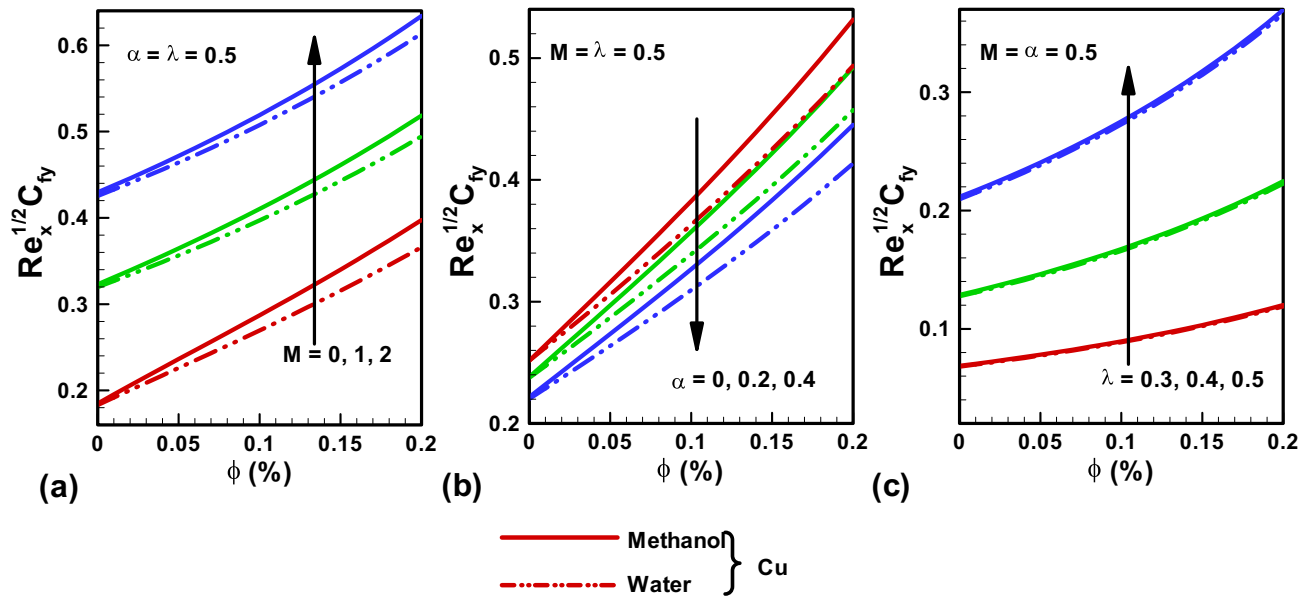


Figure 6. Skin friction results along y-direction (a) variable M . (b) variable α . (c) variable λ . Red, Blue, Green Solid lines are for Methanol, Red, Blue, Green dotted lines are for water.

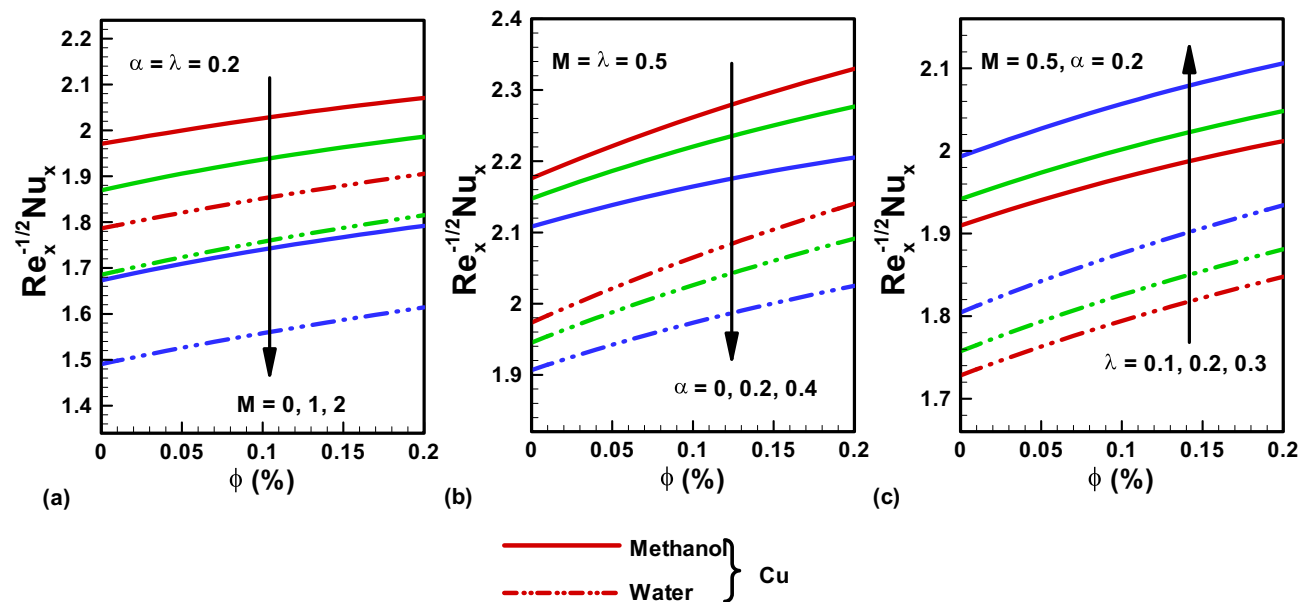


Figure 7. Nu results for (a) M (b) α . (c) λ . Red, Blue, Green Solid lines are for Methanol, Red, Blue, Green dotted lines are for water.

extent of thermal boundary layer is observed with increasing Hartmann number M . Because when we increase the Hartmann number electromagnetic force will be dominant to the viscous forces that will raise the boundary layer thickness. The incrementing values of temperature viscosity parameter α produce some high fluid resistance and it eventually adds up to a high temperature profile. Thus, an enhanced thermal boundary layer is observed.

Figure 5a–c provide the graphical solutions of skin-friction for multiple flow parameters like M, α, λ . Figure 6a–c convey the two distinct considered cases with water and Methanol base fluids. A higher value of skin friction is noted for Methanol in comparison to water. A rise in skin friction is revealed for both cases of base fluid with incrementing M . Because when we increase the Hartmann number, the electromagnetic force will be dominant to the viscous forces that will increase the skin friction. Further for both cases of water and Methanol as base fluids, an enhancement in skin friction is noted for enhancing values of the temperature dependent viscosity parameter α . As increasing temperature dependent viscosity parameter α enhance the fluid resistance that will enhance the skin friction coefficient. Further increasing values of α decreases skin friction coefficient both in x and y directions. The high values of ratio of stretching velocities in the y- and x-directions λ also result in enhancing skin friction values for both base fluid cases.

Physical properties	Base fluid		Nanoparticles
	Water	Methanol	Copper
ρ (kg/m ³)	997	792	8933
c_p (J/kg K)	4179	2545	385
k (W/m K)	0.613	0.2035	401
Pr	6.2	7.38	–

Table 1. Thermophysical properties of base fluids and copper.

M	$-g''(0)$		
	Present results	Nadeem et al. ³⁵	Wang ²⁵
0	1.173721	1.1748	1.173720
10	3.367240	3.3667	–
100	10.066473	10.0663	–

Table 2. Skin friction outcomes comparison for pure fluid with $\alpha = 0$ and $\lambda = 1$.

Pr	ϕ	Wang ²⁵	Liu et al. ³⁹	Nadeem et al. ³⁵	Present work
1	0	0.27741	0.27741	0.27741	0.27741
	0.1	– 0.4496	– 0.4496	– 0.4496	– 0.4496
	0.3	– 0.8547	– 0.8547	– 0.8547	– 0.8547
	0.4	– 1.4602	– 1.4602	– 1.4602	– 1.4602
5	0	1.3532	1.3532	1.3532	1.3532
	0.1	– 1.4212	– 1.4212	– 1.4212	– 1.4212
	0.3	– 1.7001	– 1.7001	– 1.7001	– 1.7001
	0.4	– 1.8021	– 1.8021	– 1.8021	– 1.8021

Table 3. Heat transfer rate outcomes comparison for pure fluid with $\alpha = 0$ and $\lambda = 1$, $M = 0$.

Figure 7a–c highlight the graphical illustrations on Nusselt number for multiple parameters. A higher value of Nu is noted for Methanol in comparison to water. Figure 7a depicts a decline in the Nusselt number with rising values of M for both base fluid cases. Thus, Nu declines when a high magnetic field is working as compared to viscous effects. Figure 7b shows that the numerical values of Nu decline for incrementing α . An increase in the value of Nu is observed for incrementing λ as depicted in Fig. 7c. The thermo physical properties of base fluids and Copper are presented in Table 1. Tables 2 and 3 gives the comparison of the present work with existing literature.

Conclusion

A three-dimensional flow analysis is provided for the MHD effects on nanofluids flow over a stretchable surface. This model is applicable in engineering and industrial applications, especially in paper printing and paper production. The numerical solutions are provided for the present research. Some prime outcomes are presented here as:

1. The velocity boundary thickness in x- and y- directions are altered by changes of M , ϕ and α .
2. The extent of thermal boundary layer is also augmented by the rising effect of M and α .
3. The coefficient of skin friction in both the x- and y- directions are having relevant changes in magnitude for M , α and λ .
4. The coefficient of skin friction is more for Methanol base fluids in comparison to water base fluid.
5. Nusselt number is rehabilitated with variations in magnetic field, viscosity parameter.
6. Nusselt number is high for Methanol base fluids compared to water base fluid.

Data availability

The data sets used and/or analyzed during the current study can be made available from the corresponding author on reasonable request.

Received: 28 December 2022; Accepted: 20 February 2023

Published online: 24 February 2023

References

- Das, S. K., Choi, S. U. & Patel, H. E. Heat transfer in nanofluids: A review. *Heat Transf. Eng.* **27**(10), 3–19 (2006).
- Wang, X. Q. & Mujumdar, A. S. Heat transfer characteristics of nanofluids: A review. *Int. J. Therm. Sci.* **46**(1), 1–19 (2007).
- Trisaksri, V. & Wongwises, S. Critical review of heat transfer characteristics of nanofluids. *Renew. Sustain. Energy Rev.* **11**(3), 512–523 (2007).
- Murshed, S. M. S., Leong, K. C. & Yang, C. Thermophysical and electrokinetic properties of nanofluids: A critical review. *Appl. Therm. Eng.* **28**(17), 2109–2125 (2008).
- Wang, X. Q. & Mujumdar, A. S. A review on nanofluids—part I: Theoretical and numerical investigations. *Braz. J. Chem. Eng.* **25**(4), 613–630 (2008).
- Kakac, S. & Pramuanjaroenkij, A. Review of convective heat transfer enhancement with nanofluids. *Int. J. Heat Mass Transf.* **52**(13), 3187–3196 (2009).
- Wen, D., Lin, G., Vafaei, S. & Zhang, K. Review of nanofluids for heat transfer applications. *Particuology* **7**(2), 141–150 (2009).
- Yu, W. & Xie, H. A review on nanofluids: Preparation, stability mechanisms, and applications. *J. Nanomater.* **1**, 1–10 (2012).
- Kumar, K. A., Sugunamma, V. & Sandeep, N. Effect of thermal radiation on MHD Casson fluid flow over an exponentially stretching curved sheet. *J. Therm. Anal. Calorim.* **140**, 2377–2385 (2020).
- Taylor, R. *et al.* Small particles, big impacts: A review of the diverse applications of nanofluids. *J. Appl. Phys.* **113**(1), 011301 (2013).
- Kumar, K. A., Sugunamma, V. & Sandeep, N. Simultaneous solutions for first order and second order slips on micropolar fluid flow across a convective surface in the presence of Lorentz force and variable heat source/sink. *Sci. Rep.* **9**, 14706 (2019).
- Sarkar, J., Ghosh, P. & Adil, A. A review on hybrid nanofluids: Recent research, development and applications. *Renew. Sustain. Energy Rev.* **43**, 164–177 (2015).
- Kumar, K. A., Sandeep, N. & Sugunamma, V. Influence of viscous dissipation on MHD flow of micropolar fluid over a slendering stretching surface with modified heat flux model. *J. Therm. Anal. Calorim.* **139**(4), 3661–3674 (2020).
- Akbar, N. S., Tripathi, D., Khan, Z. H. & Bég, O. A. A numerical study of magnetohydrodynamic transport of nanofluids over a vertical stretching sheet with exponential temperature-dependent viscosity and buoyancy effects. *Chem. Phys. Lett.* **661**, 20–30 (2016).
- Akbar, N. S., Maraj, E. N., Noor, N. F. M. & Habib, M. B. Exact solutions of an unsteady thermal conductive pressure driven peristaltic transport with temperature-dependent nanofluid viscosity. *Case Stud. Therm. Eng.* **35**, 102124 (2022).
- Sheikholeslami, M. & Chamkha, A. J. Electrohydrodynamic free convection heat transfer of a nanofluid in a semi-annulus enclosure with a sinusoidal wall. *Numer. Heat Transf. A* **69**(7), 781–793 (2016).
- Uddin, M. J., Kabir, M. N. & Bég, O. A. Computational investigation of Stefan blowing and multiple-slip effects on buoyancy-driven bioconvection nanofluid flow with microorganisms. *Int. J. Heat Mass Transf.* **95**, 116–130 (2016).
- Sheikholeslami, M. & Chamkha, A. J. Flow and convective heat transfer of a ferro-nanofluid in a double-sided lid-driven cavity with a wavy wall in the presence of a variable magnetic field. *Numer. Heat Transf. A* **69**(10), 1186–1200 (2016).
- Kothandapani, M. & Prakash, J. Influence of thermal radiation and magnetic field on peristaltic transport of a newtonian nanofluid in a tapered asymmetric porous channel. *J. Nanofluids* **5**(3), 363–374 (2016).
- Akbar, N. S. & Habib, M. B. New trends of nanofluids to combat *Staphylococcus aureus* in clinical isolates. *J. Therm. Anal. Calorim.* **143**, 1893–1899 (2021).
- Basir, M. F. M., Uddin, M. J., Ismail, A. M. & Bég, O. A. Nanofluid slip flow over a stretching cylinder with Schmidt and Péclet number effects. *AIP Adv.* **6**(5), 055316 (2016).
- Sheikholeslami, M., Rashidi, M. M., Hayat, T. & Ganji, D. D. Free convection of magnetic nanofluid considering MFD viscosity effect. *J. Mol. Liq.* **218**, 393–399 (2016).
- Tripathi, D., Bhushan, S., Bég, O. A. & Akbar, N. S. Transient peristaltic diffusion of nanofluids: A model of micropumps in medical engineering. *J. Hydrodyn. B* **30**, 1001–1011 (2018).
- Akbar, N. S., Shoaib, T. D., Bhushan, S. & Bég, O. A. A study of entropy generation and heat transfer of CNT-nanofluids in flow driven by beating cilia through porous medium. *J. Hydrodyn. B* **30**, 296–306 (2018).
- Wang, C. Y. The three-dimensional flow due to a stretching flat surface. *Phys. Fluids* **27**(8), 1915 (1984).
- Hayat, T., Muhammad, T., Shehzad, S. A. & Alsaedi, A. Three-dimensional flow of Jeffrey nanofluid with a new mass flux condition. *J. Aerosp. Eng.* **29**(2), 04015054 (2015).
- Mahanthesh, B., Gireesha, B. J. & Gorla, R. S. R. Nanoparticles effect on 3D flow, heat and mass transfer of nanofluid with nonlinear radiation, thermal-diffusion and diffusion-thermo effects. *J. Nanofluids* **5**(5), 669–678 (2016).
- Kolsi, L. *et al.* 3D buoyancy-induced flow and entropy generation of nanofluid-filled open cavities having adiabatic diamond shaped obstacles. *Entropy* **18**(6), 232 (2016).
- Khan, J. A., Mustafa, M. & Mushtaq, A. On three-dimensional flow of nanofluids past a convectively heated deformable surface: A numerical study. *Int. J. Heat Mass Transf.* **94**, 49–55 (2016).
- Khan, M., Khan, W. A. & Alshomrani, A. S. Non-linear radiative flow of three-dimensional Burgers nanofluid with new mass flux effect. *Int. J. Heat Mass Transf.* **101**, 570–576 (2016).
- Zhu, X. W., Fu, Y. H., Zhao, J. Q. & Zhu, L. Three-dimensional numerical study of the laminar flow and heat transfer in a wavy-finned heat sink filled with Al₂O₃/ethylene glycol-water nanofluid. *Numer. Heat Transf. A* **69**(2), 195–208 (2016).
- Raju, C. S. & Sandeep, N. Heat and mass transfer in 3D non-Newtonian nano and ferro fluids over a bidirectional stretching surface. *Int. J. Eng. Res. Africa* **21**, 33–51 (2016).
- Babu, M. J. & Sandeep, N. 3D MHD slip flow of a nanofluid over a slendering stretching sheet with thermophoresis and Brownian motion effects. *J. Mol. Liq.* **222**, 1003–1009 (2016).
- Sulochana, C., Ashwinkumar, G. P. & Sandeep, N. Similarity solution of 3D Casson nanofluid flow over a stretching sheet with convective boundary conditions. *J. Nigerian Math. Soc.* **35**(1), 128–141 (2016).
- Nadeem, S., Haq, R. U. & Khan, Z. H. Heat transfer analysis of water-based nanofluid over an exponentially stretching sheet. *Alex. Eng. J.* **53**(1), 219–224 (2014).
- Li, P., Huang, X. & Zhao, Y.-P. Active control of electro-visco-fingering in Hele-Shaw cells using Maxwell stress. *Science* **25**, 105204 (2022).
- Huang, X., Dong, H., Liu, Z. & Zhao, Y.-P. Probing micro-newton forces on solid/liquid/gas interfaces using transmission phase shift. *Langmuir* **35**, 5442–5447 (2019).
- Disu, A. B. & Dada, M. S. Reynold's model viscosity on radiative MHD flow in a porous medium between two vertical wavy walls. *J. Taibah Univ. Sci.* **11**, 548–565 (2017).
- Liu, C., Wang, H.-H. & Peng, Y.-F. Flow and heat transfer for three-dimensional flow over an exponentially stretching surface. *Chem. Eng. Commun.* **200**, 253–268 (2013).
- Venkata Ramudu, A. C., Kumar, K. A., Sugunamma, V. & Sandeep, N. Impact of Soret and Dufour on MHD Casson fluid flow past a stretching surface with convective–diffusive conditions. *J. Therm. Anal. Calorim.* **147**, 2653–2663 (2022).

Acknowledgements

The authors extend their appreciation to the Deanship of Scientific Research at King Khalid University for funding this work through research groups program under Grant No. R.G.P2/172/43.

Author contributions

All authors listed have made a substantial, direct, and intellectual contribution to all the section of the manuscript .

Competing interests

The authors declare no competing interests.

Additional information

Correspondence and requests for materials should be addressed to N.S.A.

Reprints and permissions information is available at www.nature.com/reprints.

Publisher's note Springer Nature remains neutral with regard to jurisdictional claims in published maps and institutional affiliations.



Open Access This article is licensed under a Creative Commons Attribution 4.0 International License, which permits use, sharing, adaptation, distribution and reproduction in any medium or format, as long as you give appropriate credit to the original author(s) and the source, provide a link to the Creative Commons licence, and indicate if changes were made. The images or other third party material in this article are included in the article's Creative Commons licence, unless indicated otherwise in a credit line to the material. If material is not included in the article's Creative Commons licence and your intended use is not permitted by statutory regulation or exceeds the permitted use, you will need to obtain permission directly from the copyright holder. To view a copy of this licence, visit <http://creativecommons.org/licenses/by/4.0/>.

© The Author(s) 2023